PROCEEDINGS, Thirty-Third Workshop on Geothermal Reservoir Engineering
Stanford University, Stanford, California, January 28-30, 2008
SGP-TR-185

TRACER TEST ANALYSIS WITH TRIPLE POROSITY MODEL FOR NATURALLY FRACTURED RESERVOIRS WITH TRANSIENT TRANSFER IN MATRIX-FRACTURE AND MICROFRACTURES-FRACTURES

Héctor Pulido[1], Fernando Samaniego V.[1,] Jesús Rivera R.[1], Guadalupe Galicia-Muñoz[1] and Carlos Vélez[1]

1. National University of Mexico, 2. PEMEX

ABSTRACT

This paper presents a new model and its solution for the flow of tracers in reservoirs, both radioactive and chemical, under constant mass flux conditions, which can be used for the design, evaluation and interpretation of injection tests. The models developed consider homogeneous and naturally fractured reservoirs (NFR). For the case of NFR, a transient fracture-matrix tracer transfer is assumed. The transient between two porous media is modeled in a convolution form and using a skin form to obtain a pseudosteady state behavior. The models and the solutions acquired include the tracer lost to the matrix inaccessible (dead end) pore volume. The dimensionless groups used in this work resemble as much as possible those used in well test analysis.

Short and long time approximate analytical solutions for these tracer flow conditions are derived, which are useful to validate the general Laplace space solution, and for the interpretation of the tracer response in observation wells.

The solutions presented in this work were applied to a real field interwell (observation) tracer response, allowing the estimation of important fluid and reservoir parameters, such as the radial dispersion coefficient, D_r, and for NFR the average fracture aperture (width) and the block size.

The evaluation and interpretation of a pulse tracer test in a complex naturally fractured and stratified carbonate reservoir, is evaluated and analyzed. In this test a chemical tracer Perfluoromethylcyclopentane (PMCP) was used.
.

INTRODUCTION

Tracers are substances that are added to the injected fluid with the purpose of studying the trajectory of the fluids inside a reservoir, as they advance toward the producing wells. A tracer should meet certain characteristics, among others: not interfere with the fluid flow, require a small concentration and easy detection. Another purpose of introducing a tracer in the injected fluid is to detect the fractures preferential orientation or discontinuities in the reservoir. In any project of fluid injection, the channels of high permeability in the reservoir can quickly establish "short-circuits" for the injected fluid, reducing the efficiency of the process drastically, and in some cases can cause the failure of the project. The field tests with well to well tracer injection and the data analysis with the correct model, provide the possibility for the improvement of the reservoir characterization.

The information that is possible to obtain from well to well tracer tests is the following: sweep| efficiency, identification of high permeability zones, inadequate injectors wells, preferential flow tendencies, location of barriers, relative velocity of the injected fluids, and in general the trajectories of the fluids injected into the reservoir toward the producing wells. Tracers that have been successfully used in the industry are: tritiated methane, ammonium nitrate, isopropilic alcohol, thorium, tritium, deuterium, krypton 85, iodide and strontium. These tracers have fulfilled the international norms of security.

Tracers such as tritium and krypton 85 emit beta radiation, and can be detected using a highly sensitive proportional counter, in concentrations as low as of one picocurie/liter. Tritium in water is detected using a Geiger counter coupled with wireline. With respect to chemical tracers, these must be used in high concentrations, are relatively most expensive and easily detectable. The perfluorinated molecules are of great interest as gas tracers. SF6 has been used with success for many years. The focus has been put on perfluorinated cyclic molecules, like perfluorodimethylcyclobutane (PDMCB) and, perfluoromethylcyclopentane; these are commonly named PFTs. The PFTs are non toxic products, low-cost and with an exceptionally low detection limit with Geiger counters. The first field injection of PFTs was carried out in the Ekofisk field in the North Sea in 1987, on a trial-and error basis[1]. The mass of tracer injected depends among other factors on the travel distance, half life, degree of adsorption in the rock, high permeability channels (short circuits), formation temperature, peak

concentration, dispersivity constant, magnitude of the inaccessible pore volume, etc.[2]

The injection of a tracer in a naturally fractured reservoirs, allows through a solution of the mathematical models that describe these flow problems, the interpretation of the response in producers wells; as a result we can estimate parameters of practical interest.

The purpose of this study is to present a new model with transient fracture-matrix transfer, for the tracer response in the producing wells, considering the continuous injection of a tracer. The main contributions of this work consist in taking into account radioactive decay, the inaccessible matrix pore volume, the definition of a dimensionless radius similar to that used in well test analysis (instead of the traditional one that is referred to the mixing coefficient [dispersivity]), the dimensionless time associated with the dispersion coefficient, the approximate analytical solutions for short and long dimensionless times, and a type curve that allows the estimation of the radial dispersion coefficient (D_r).

MODELS PREVIOUSLY PRESENTED FOR TRACER FLOW

Study of the tracer dispersion in naturally fractured reservoirs is of growing interest for the characterization of a reservoir, mainly due to the current importance of fluid injection projects to improve the recovery of hydrocarbons. The dispersion effect controls the success of a tracer injection process. In the past, several papers have discussed the theory related to the flow of tracers in porous media. Raimondi et al.[3], presented an approximate solution for the flow of a chemical tracer flow under radial flow conditions. A complete revision was presented by Perkins and Johnston[4], as well as Pozzi and Blackwell[5]. Bentsen and Nielsen[6] presented laboratory data for radial systems, and showed that the tracer dispersion behavior can be appropriately described by means of the solution of Raimondi et al., when the mobility relationship is favorable. Brigham and Smith[7] applied the solution of Raimondi et al. to predict the behavior of a chemical tracer in a five spot pattern. Yuen, Brigham and Cinco[8], presented a methodology to predict the radial flow behavior of a chemical tracer in a stratified reservoir, where the response showed peaks depending on the strata characteristics. Tang and Babu[9] presented a solution for the radial dispersion problem in terms of fractionary modified Bessel functions. Moench and Ogata[10], presented a solution in Laplace space for chemical tracer radial flow in terms of Airy functions, and obtained the numerical inversion with the algorithm of Stehfest[11], and through a finite difference solution. Later, Abbaszadeh and Brigham[12], continued the work of Yuen et. al. to determine stratified characteristics. Hsieh[13], presented the solution to the problem of Moench and Ogata, expressed in terms of an integral in the complex plane.

Chen[14], presented analytical solutions for radial dispersion with Cauchy boundary at injection well, using the dispersivity in similar form as the skin in the injection well.

Ramírez[15], obtained a solution in Laplace space for the radial flow of tracers in naturally fractured reservoirs, and carried out the inversion of their Laplace space solution with Crump's algorithm[16], coupled with Epsilon's algorithm for acceleration. They considered slabs and cubic models for the matrix-fracture geometry.

Pulido[17] and Pulido et al.[18], presented analytical solution for the radial dispersion problem for homogeneous and naturally fractured reservoirs, taking into account the radioactive decay, using the dimensionless time based on the dispersion coefficient, and observed that for large time the solution for constant concentration is under steady-state conditions.

Samaniego et al.[19] were focused in apply the theory in a field data for characterization naturally fractured reservoirs.

MODELS PROPOSED MATHEMATICAL MODEL

With the purpose of allowing a mathematical analysis of the tracer flow problem, it is necessary to model the real system, irregular and complex, composed of matrix and fractures, by matrix blocks that have the same size and form (Fig. 1). A percentage of the connected pore volume in naturally fractured reservoirs is not accessible to injection; thus changes are required to include inaccessible pore volume in the mathematical models, because it affects tracer propagation significantly.

The double porosity model proposed in this work considers the following assumptions:

1. The matrix and fractures are homogeneous and compressible systems.
2. Fluid is injected across the fractures and then flows from the fractures to matrix.
3. There is not resistance to flow between the fracture and matrix **(Fig. 2)**.
4. The matrix-fracture geometries considered are slabs and cubic blocks **(Fig. 1)**.
5. Injection of mass flux is constant and uniformly distributed over the interval.
6. Fracture width is small compared with that of the matrix block.

7. The effective diffusivity coefficient in the matrix is constant, and in the fractures the longitudinal dispersion coefficient is proportional to the radial velocity.
8. Diffusion in the fractures and in the matrix obeys Fick's law.
9. A uniform vertical z direction gradient concentration exists in the fractures.
10. The porous media are of finite extent.

Under the previous assumptions, the equation for the radial flow of tracers in naturally fractured reservoirs can be expressed:

$$\frac{1}{r}\frac{\partial}{\partial r}\left(rD_r \frac{\partial C_f(r,t)}{\partial r} \right) - v_r \frac{\partial C_f(r,t)}{\partial r} - \lambda C_f(r,t)$$

$$- \frac{J_{mf}(h_f,t)}{\phi_{fb}\sigma_{mf}} - \frac{J_{mff}(h_{mf},t)}{\phi_{mfb}\sigma_{mf}} = \frac{\partial C_f(r,t)}{\partial t}. \qquad (1)$$

The longitudinal dispersion coefficient and radial velocity are expressed by Eqs. (2) and (3):

$$D_r = \alpha v_r; \qquad (2)$$

$$v_r = \frac{q}{2\pi r h} = \frac{a_f}{r}. \qquad (3)$$

Combining Eqs. (2) and (3):

$$rD_r = \alpha a_f. \qquad (4)$$

Substituting Eqs. (3) and 4 in Eq. (1), the equation for the radial flow of tracers in naturally fractured reservoirs is obtained:

$$\frac{\alpha a_f}{r}\frac{\partial^2 C_f(r,t)}{\partial r^2} - \frac{a_f}{r}\frac{\partial C_f(r,t)}{\partial r} - \lambda C_f(r,t)$$

$$- \frac{J_{mf}(h_f,t)}{\phi_{fb}\sigma_{mf}} - \frac{J_{mmf}(h_{mf},t)}{\phi_{mfb}\sigma_{mff}} = \frac{\partial C_f(r,t)}{\partial t}, \qquad (5)$$

where the tracer mass transfer by matrix and microfractures rock volume unit $J_{mf}(h_f,t)$ is given by Eq. (6):

$$J_{mf}(h_f,t) = \frac{D_m}{V_b}\frac{\partial C_m(h_f,t)}{\partial z}, \qquad (6)$$

$$J_{mff}(h_{mf},t) = \frac{D_m}{V_b}\frac{\partial C_m(h_{mf},t)}{\partial z} \qquad (6')$$

and the interporosity shape factor:

$$\sigma_{mf} = \frac{12}{H^2}, \qquad (7)$$

$$\sigma_{mff} = \frac{12}{h_{mf}^2}, \qquad (7')$$

Substituting Eq. in Eq. (5), the equation for the radial flow of tracers in naturally fractured reservoirs can be expressed as follows:

$$\frac{\alpha a_f}{r}\frac{\partial^2 C_f(r,t)}{\partial r^2} - \frac{a_f}{r}\frac{\partial C_f(r,t)}{\partial r} - \lambda C_f(r,t)$$

$$+ \frac{D_m}{\phi_{fb}\sigma_{mf}V_b}\frac{\partial C_m(h_f,t)}{\partial z} + \frac{D_m}{\phi_{mfb}\sigma_{mff}V_b}\frac{\partial C_{mf}(h_{mf},t)}{\partial z} = \frac{\partial C_f(r,t)}{\partial t} \qquad (8)$$

It is important to notice that in the left-hand side of Eq. (8) the first term refers to the tracer transfer by *dispersion*, the second to the concentration change of tracer due to the *convection*, the third to the *radioactive decay*, and the fourth term refers to *fracture-matrix transfer*, where the new interporosity flow coefficient governs the tracer flow to the matrix, and therefore controls the time period of the transition between the early tracer flow only through the fractures, to the composite by fractures and matrix tracer flow. The right-hand side member of Eq. (8) considers the tracer concentration change with time, that represents the cumulative effect.

The equation for the linear flow in the matrix, taking into account the inaccessible pore volume:

$$D_m\frac{\partial^2 C_m(z,t)}{\partial z^2} - \lambda C_m(z,t) - (1-f)\frac{\partial C_{sm}(z,t)}{\partial t}$$

$$= f\frac{\partial C_m(z,t)}{\partial t}. \qquad (9)$$

In Eq. (9) the first term on the left-hand side refers to the tracer transfer by *diffusion*, the second to the *radioactive decay*, and the third term represents the *loss* of tracer to the inaccessible pore volume; the right member of Eq. (9) considers the concentration change with the time, that represents the *cumulative* effect.

Transfer between the two zones in the matrix, the active and the inaccessible pore volume:

$$\frac{\partial C_{sm}(z,t)}{\partial t} = \frac{M_m}{1-f}\left[C_m(z,t) - C_{sm}(z,t) \right]. \qquad (10)$$

The dimensionless model for the radial flow of a tracer in a fractured system, is given by Eqs. (11) to (19).

Tracer flow equation:

$$\frac{1}{r_D}\frac{\partial^2 C_{fD}(r_D,t_D)}{\partial r_D^2} - \frac{1}{\alpha_D r_D}\frac{\partial C_{fD}(r_D,t_D)}{\partial r_D} - \lambda_D C_{fD}(r_D,t_D)$$

$$\frac{1}{\sigma_{mf}}\frac{\partial C_{fD}(z_{Dmf},t_D)}{\partial t_D}*\left(\frac{F_{mmf}(n_{mD},t_D)}{1+S_{mmf}F_{mmf}(n_{mD},t_D)}\right)$$

$$+\frac{1}{\sigma_{Dmff}}\frac{\partial C_{fD}(z_{Df},t_D)}{\partial t_D}*\left(\frac{F_{mf}(m_{mD},t_D)}{1+S_{mf}F_{mf}(m_{mD},t_D)}\right)=\frac{\partial C_{fD}(r_D,t_D)}{\partial t_D}\ ; \tag{11}$$

Initial condition:

$$C_{fD}(r_D,0)=0\ ; \tag{12}$$

Internal boundary condition: constant mass flux at injection well.

$$\frac{\partial C_{fD}(1,t_D)}{\partial r_D}=-1\ . \tag{13}$$

External boundary condition: infinite

$$\lim_{r_D\to\infty} C_{fD}(r_D,t_D)=0\ ; \tag{14}$$

Dimensionless tracer flow equation for linear flow in the matrix, taking into account the inaccessible pore volume:

$$D_{mD}\frac{\partial^2 C_{mD}(z_D,t_D)}{\partial {z_D}^2}-\lambda_D C_{mD}(z_D,t_D)$$

$$-(1-f)\frac{\partial C_{smD}(z_D,t_D)}{\partial t_D}=f\frac{\partial C_{mD}(z_D,t_D)}{\partial t_D}\ ; \tag{15}$$

Initial condition:

$$C_{mD}(z_D,0)=0\ . \tag{16}$$

Internal boundary condition: free interaction between fracture and matrix:

$$C_{mD}(z_{fD},t_D)=C_{fD}(r_D,t_D)\ ; \tag{17}$$

Matrix Symmetrical boundary condition: closed system.

$$\frac{\partial C_{mD}(z_{HD},t_D)}{\partial z_D}=0\ ; \tag{18}$$

Transfer between two zones in the matrix by adsorption:

$$\frac{\partial C_{smD}(z_D,t_D)}{\partial t_D}=\frac{M_{mD}}{1-f}\left[C_{mD}(z_D,t_D)-C_{smD}(z_D,t_D)\right]; \tag{19}$$

Initial condition:

$$C_{smD}(z_D,0)=0\ . \tag{20}$$

Dimensionless variables.

Dimensionless radius:

$$r_D=\frac{r}{r_w}\ ; \tag{21}$$

Dimensionless time:

$$t_D=\frac{D_r\,t}{{r_w}^2}=\frac{\alpha\,v_r\,t}{{r_w}^2}=\frac{\alpha_D\,a_f\,t}{{r_w}^2}\ . \tag{22}$$

Dimensionless length in the matrix:

$$z_D=\frac{z}{r_w}\ . \tag{23}$$

Dimensionless fracture half width **(Fig. 2)**:

$$z_{fD}=\frac{h_f}{r_w}\ . \tag{24}$$

$$z_{mfD}=\frac{h_{mf}}{r_w}\ . \tag{25}$$

Dimensionless (symmetrical) maximum distance for tracer flow in the matrix:

$$z_{HD}=\frac{H+h_f}{r_w}\ . \tag{26}$$

Dimensionless tracer concentration in the fractures:

$$C_{fD}(r_D,t_D)=\frac{2\pi hD_r}{\dot{m}_w}C_f(r,t)\ , \tag{27}$$

where $\dot{m}_p$ is defined by Eq. (A-5).

Dimensionless tracer concentration in the matrix:

$$C_{mD}(z_D,t_D)=\frac{2\pi hD_r}{\dot{m}_w}C_m(z,t)\ . \tag{28}$$

Dimensionless tracer concentration in the matrix inaccessible pore volume:

$$C_{smD}(z_D,t_D)=\frac{2\pi hD_m}{\dot{m}_w}C_{sm}(z,t)\ . \tag{29}$$

Dimensionless mixing coefficient (dispersivity):

$$\alpha_D=\frac{\alpha}{r_w}\ . \tag{30}$$

Dimensionless interporosity coefficient:

$$\sigma_{Dmf}=\frac{\alpha_D a_f \phi_{fb}\sigma V_b}{D_m r_w}=\frac{D_r \phi_{fb}\sigma V_b}{D_m r_w}\ . \tag{31}$$

$$\sigma_{Dmff}=\frac{\alpha_D a_{mf} \phi_{fb}\sigma V_b}{D_m r_w}=\frac{D_r \phi_{fb}\sigma V_b}{D_m r_w}\ . \tag{31'}$$

Fracture porosity:

$$\phi_{fb}=\frac{h_f}{3H}\ . \tag{32}$$

Microfracture porosity:

$$\phi_{mfb} = \frac{h_{mf}}{3H}. \qquad (32')$$

Dimensionless effective diffusivity in the matrix:

$$D_{mD} = \frac{D_m}{\alpha_D a_f}. \qquad (33)$$

Dimensionless adsorption coefficient for the inaccessible pore volume:

$$M_{mD} = \frac{M_m r_w^{\,2}}{\alpha_D a_f}. \qquad (34)$$

Dimensionless radioactive decay constant:

$$\lambda_D = \frac{r_w^{\,2}\lambda}{\alpha_D a_f}. \qquad (35)$$

SOLUTION FOR AN INFINITE SYSTEM

The wellbore concentration in Laplace space for the problem considered is (see Appendix A):

$$\overline{C}_{wD}(s) = \frac{-1}{s\left[0.5\alpha_D + (\beta(s))^{1/3} A_i'(Y_1)/A_i(Y_1)\right]}. \qquad (36)$$

For enlarged microfractures:

$$\beta_1(s) = \frac{\sqrt{s\,m(s)}}{\sigma_D}\left[\frac{tgh\left(z_{HD}\sqrt{s\,m(s)}\right) - tgh\left(z_{fD}\sqrt{s\,m(s)}\right)}{1 - tgh\left(z_{HD}\sqrt{s\,m(s)}\right) tgh\left(z_{fD}\sqrt{s\,m(s)}\right)}\right] \qquad (37)$$

For cubic matrix:

$$\beta_2(s) = \frac{\sqrt{s\,m(s)}}{\alpha_D \sigma_D}\left[coth\left(\sqrt{s\,m(s)}\, z_{Df}\right) - \frac{1}{z_{Df}\sqrt{s\,m(s)}}\right] \qquad (38)$$

Now, there are two sources in the transfer functions

$$\beta(s) = \beta_1(s) + \beta_2(s) + \lambda_D + s; \qquad (38')$$

and y_0, y_1 and $m(s)$ for both matrix geometries are given by Eqs. 39 and 40:

$$Y_0 = \frac{1/4\alpha_D^{\,2}}{(\beta(s))^{2/3}}. \qquad (39)$$

$$Y_1 = \frac{\beta(s) + 1/4\alpha_D^{\,2}}{(\beta(s))^{2/3}}; \qquad (40)$$

$$m(s) = \frac{1}{D_{mD}}\left[\frac{(1-f)M_{mD}}{M_{mD} + s(1-f)} + f + \frac{\lambda_D}{s}\right]. \qquad (41)$$

Approximate analytical solution infinite for short times

During the early injection phase when a small pore volume has been injected, the fracture-matrix tracer mass transfer is negligible, and the naturally fractured formation behaves as a "homogeneous in fractures media". Thus for short dimensionless times, it is possible to invert Eq. (E-17) (see Appendix E):

$$C_{wD}(t_D) = 0.432 t_D^{\,11/9} \qquad (42)$$

Approximate analytical solution for long times

For long dimensionless times, the solution for the radial flow of a radioactive tracer in naturally fractured reservoirs, Eqs. (36) and (E-18) (see Appendix E), can be expressed as follows:

$$C_{wD}(t_D) = 0.4\alpha_D^{\,2} t_D^{\,1/3} \qquad (43)$$

These solutions given by Eqs. (45) and (46) were used in the present work to test the validity of the numerical inversion results.

Derivation of the dimensionless groups

If the analytical solution for short times for the continuous radial flow of a radioactive tracer given by Eq. (45), is derived with respect to time t_D and multiplied by t_D, a useful way to present the results of this problem is obtained in terms of:

$$t_D \frac{dC_{wD}(t_D)}{dt_D} \quad vs. \quad t_D. \qquad (44)$$

The solution have the form

$$C_{wD}(t_D) = A t_D^{\,n} \qquad (45)$$

The derivative with respect to time:

$$\frac{dC_{wD}(t_D)}{dt_D} = [n-1] A t_D^{\,n-1} \qquad (46)$$

Multiply by the time:

$$t_D \frac{dC_{wD}(t_D)}{dt_D} = [n-1] A t_D^{\,n} \qquad (47)$$

Both:

$$t_D \frac{dC_{wD}(t_D)}{dt_D} = \frac{dC_{wD}(t_D)}{d\ln t_D} \qquad (48)$$

The logarithmic derivatitive must be the same form:

$$\frac{dC_{wD}(t_D)}{d\ln t_D} = [n-1] A t_D^{\,n} \qquad (49)$$

$$\frac{dC_{wD}(t_D)}{d\ln t_D} = [0.4/3]\alpha_D^{\,2} t_D^{\,1/3} \qquad (50)$$

The behavior of concentration show two straight lines, which derivatives are parallel and allow identify the radial flow, when match the dimensionless solution to

data in a log-log graph is obtained the dimensionless mixing coefficient.
Allows to compare the value obtained in laboratory with field test and including in the numerical model of reservoir for optimization exploitation, enhanced recovery or secondary process.

The results of several fisycal. such as Jogen et al.20 show that is possible to represent the behavior of hydrodynamical dispersion using fractals, experimentally, by numerical simulations, in others words, the exponent of the time is fraction, without geometrical regular representation, in reality is a ratio of density of one media inside other.

Solutions for constant Mass Flux Pulse
For instance, if a well is injected for a time Δt, then shut in, by superposition in time, the concentration response in the shut in well is:

$$C_{wD}(t_D) = 0.4\alpha_D{}^2\left[t_D{}^{1/3} - (t_D - \Delta t_D)^{1/3}\right] \quad (51)$$

Numerical inversion
The comparison between the numerical inversion with Stehfest's algorithm and the approximate analytical solutions for short and long dimensionless times (not shown in this paper), indicates that the numerical solution is correct. **Figs. 2** and **3** were generated through numerical inversion using the algorithm of Stehfest[11]. **Fig**. **3** shows in addition to the tracer response a graph of its logarithmic derivative.

Numerical inversion has the advantage that the calculation time is smaller than the simulation time using finite differences. In addition, it has been concluded that the numerical inversion is efficient for any boundary condition.

The derivative of the solution for continuous injection is a solution for the pike injection.

Tracer test conducted during nitrogen injectivity test.
It was decided to inject a tracer during a short-term nitrogen injection test conducted at well T-428 from the Jujo-Tecominoacan field, Mexico, **Fig.7** , in order to determine if natural fractures trends suspected to exist within the test area, would have some effect on the flow of injected nitrogen at reservoir conditions. Total cumulative injected volume was 0.455 x 10^6 m^3 during 26 h. Nitrogen was injected at three increasing flow rates of 5.01, 15.17 and 19.91 *MMscf / D*. A perfluorocarbon chemical tracer (PMCP) was added to the main nitrogen stream; tracer response within 1 to 2 days was observed in four observation wells, as shown in Table 1 and **Fig. 8** and **9**. Distances of observers to the injection well ranged from 436 to 822 m, while breakthrough times varied from 1 to 2 days. Taking into account these figures, "apparent superficial velocities" between 323 and 436 m/day can be calculated for the flow of the injected tracer between each pair of wells, as shown in Table 2.

Table 1. Breakthrough times for the injected tracer, including measured tracer concentrations.

Well	Distance to injector, m	Breakthrough time, days	Tracer concentration, ppb
120	646	2	1.4
408	810	2	0.9
429	436	1	0.9
446	822	2	1.1

It can be seen from Figure **7**, that arrival of several tracer pulses at the observation wells can be suspected from the shape of the tracer response curve. Using the peak concentrations from each one of three possible tracer pulses, apparent superficial velocities for each of them can be calculated, as shown in Table 2.

Table 2. Average tracer apparent superficial velocities, based upon maximum pulse tracer concentrations arrival times, Jujo-Tecominoacán, field, Mexico.

Well	First pulse		Second pulse		Third pulse	
	t_{max}, days	v, m/day	t_{max}, days	v, m/day	t_{max}, days	v, m/day
120	2	323	5	129	7	92
408	2	405	5	162	7	116
429	1	436	5	87	7	62
446	2	411	5	164	6.5	126

Based upon results obtained from tracer flow, it was concluded that a clear indication existed that natural fractures were communicating the injection well and the four observation wells included in Tables 1 and 2. Furthermore, considering the shape of the tracer response curve, it could be inferred that tracer moved preferentially through several systems of high fluid conductivity trends acting in parallel, which showed as several tracer pulses arriving at different times to a given observation well. Reservoir volumes associated to these highly conductive paths, were small compared to total reservoir volume within the injection pattern. Knowledge of these features is very important to properly design any reservoir fluid injection project.

RESULTS, OBSERVATION AND CONCLUSIONS

This study discussed two new models and their solutions for the flow of tracers in homogeneous and NFR, considering the physically correct inner (injection) boundary condition at the well of constant mass flux. The solutions derived include the cases of a continuous and pulse (finite) tracer injection.

In addition, for these purposes, based on the short time previous solutions, a useful way of presenting the theoretical tracer response was developed, in terms of $t_D \partial C_{fD}(r_D, t_D)/\partial t_D$ *vs.* t_D.

TECHNICAL CONTRIBUTIONS

The main technical contributions of this paper are as follows:

1. This study presents two new models and their solutions for the flow of tracers in homogeneous and in NFR, considering the correct injection boundary condition at the well of constant mass flux.
2. A methodology for the evaluation and interpretation of a tracer injection test is discussed, which uses analytical approximate solutions, the general response graphed in terms of the convenient discussed groups and non linear regression methods.
3. The evaluation and interpretation of a field test, carried out in a Mexican oil field, are also presented in this work.

NOMENCLATURE

a = *injection constant, Eqs. 2 and 3* = $q/2\pi h$, L^2/T.
$A_i(z)$ = *Airy function.*
$B_i(z)$ = *Airy function.*
C_i = *initial tracer concentration,* M/L^3.
$C_{sm}(z,t)$ = *tracer concentration absorbed in the matrix,* M/L^3.
$C_m(z,t)$ = *tracer concentration in the matrix,* M/L^3.
$C_f(r,t)$ = *tracer concentration in the fractures,* M/L^3.
D_r = *dispersion coefficient,* L^2/T.
D_m = *effective diffusivity coefficient,* L^2/T.
f = *ratio between accessible and inaccessible porosity*
$G(r,t)$ = *mass as a function of the radial distance and time, M.*
h = *thickness of the porous media, L.*
h_f = *fracture half width, L.*
H = *half of the average matrix block size, L.*
J = *mass flux density,* M/L^2T.
J^* = *mass flux density transfer* $(M/L^3)/(L^2T)$ *by rock volume unit.*
$\dot{m}$ = *mass flux, M/T.*
M = *solute mass injected, M*
q_i = *injection flow rate in the porous media,* L^3/T.
r = *radial distance, L.*
t = *time, T*
T_0 = *delta time, T.*
U = *macroscopic velocity, L/T.*
v = *microscopic velocity, L/T.*
V_u = *fluid volume in the fracture, equal to the transfer area of the matrix block multiplied by half of the width fracture* L^3.

Greek symbols

α = α *coefficient dispersivity, L.*
$\beta(s)$ = *transfer function in Laplace space, Eqs.41 and 42.*
$\delta(t)$ = *Dirac's* δ*-function.*
ϕ = *effective porosity, dimensionless.*
λ = *radioactive decay constant, 1/T.*
κ = *mass flow gradient, 1/T.*
σ = *interporosity shape factor,* $1/L^2$.

Subscripts

b = *bulk.*
D = *dimensionless.*
f = *fracture.*
m = *matrix.*
p = *producing well.*
sm = *inaccessible matrix pore volume.*
w = *well.*

REFERENCES

1. Skilbrei, O. B., Hallenbeck, L. D. and Sylte, J. E.: "Comparison and Analysis of Radioactive Tracer Injection Response with Chemical Water Analysis into the Ekofisk Formation Pilot Waterflood", paper SPE 20776 presented at the 65th Annual Technical Conference and Exhibition, New Orleans, La., Sept. 23-26, 1990.
2. Bjornstad, T.: "New Developments in Tracer Technology for Reservoir Description", National Petroleum Show, Calgary, June 9-11, 1998.
3. Raimondi, P., Gardner, H. F. and Patrick, C. B.: "Effect of Pore Structure and Molecular Diffusion on the Mixing of Miscible Liquid Flow in Porous Media", paper No. 43 presented in the AIChE-SPE Joint Symposium on Fundamental Concepts of Miscible Displacement, Part II, San Francisco, Calif., Dec. 6-9, 1959.

4. Perkins, T. K. and Johnston, O. C.: "A Review of Diffusion and Dispersion in Porous Media", *SPE* (March, 1963) 70-84.
5. Pozzi, A. L. and Blackwell, R. J.: "Design of Laboratory Models for Study of Miscible Displacement", *SPEJ* (March, 1963).
6. Bentsen, R. G. and Nielsen, R. F.: "A Study of Radial Miscible Displacement in a Consolidated Porous Medium", *SPEJ* (March, 1965) l-5.
7. Brigham, W. E. and Smith, D. H.: "Prediction of Tracer Behavior in Five -Spot Flow", Paper SPE 1130, SPE Conference on Production Research and Engineering, Tulsa, Okla., May 3-4, 1965.
8. Yuen, D. L., Brigham, W. E. and Cinco Ley H.: "Analysis of Five Spot Tracer Tests to Determines Reservoir Layering", DOE Report SAW 1265-8 (Feb, 1979.), Washington, D. C.
9. Tang, D. H. and Babu, D. K.: "Analytical Solution of a Velocity Dependent Dispersion Problem", *Water Resources Research*, Vol. 15, No. 6. (December, 1979).
10. Moench, A. F. and Ogata, A.: "A Numerical Inversion of the Laplace Transform Solution to Radial Dispersion in Porous Media", *Water Resources Research*, Vol. 17, No.1 (February, 1981), 250-252.
11. Stehfest, H.:"Algorithm 368, Numerical Inversion of Laplace Transforms", *Communication of the ACM*, 47 (Jan., 1970) 13.
12. Abbaszadeh, M. and Brigham, W. E.: "Analysis of Well to Well Tracer Flow to Determine Reservoir Heterogeneity", (Oct., 1984), 1753-1760.
13. Hsieh, P. A.: "A New Formulation for the Analytical Solution of the Radial Dispersion Problem", *Water Resources Research*, Vol. 22, No. 11, (October, 1986) 1597-1605.
14. Chen, C-S.: "Analytical Solutions for Radial Dispersion with Cauchy Boundary at Injection Well", *Water Resources Research*, Vol. 23, No. 7 (July, 1987) 1217-1224.
15. Ramírez, S. J., Samaniego, V. F., Rivera, R. J. and Rodríguez, F.: "An Investigation of the Radial Tracer Flow in Naturally Fractured Reservoirs", Proceedings of the Sixteenth Workshop on Geothermal Reservoir Engineering, Stanford U., Stanford, Ca. (January, 1991) 23-25.
16. Crump, K. S.: "Numerical Inversion of Laplace Transforms Using Fourier Series Approximation". *J. of the Association of Computing Machinery*, Vol. 23, No.1 (January, 1976), 89-96.
17. Pulido, H.: "Modelo de Doble Porosidad para el Flujo Radial de Trazadores Radiactivos en Yacimientos Naturalmente Fracturados e Interpretación", Master Report in Petroleum Engineering, School of Engineering, National University of México, June, 2001.
18. Pulido, B. H., Samaniego, V. F., Rivera, R. J., Camacho, R., and Ramírez, S. J.: "Double Porosity Model with Transient Interporosity Flow for the Response of Tracers in Naturally Fractured Reservoirs, Considering Constant Mass Flux Injection". Proceedings of the Thirtieth Workshop on Geothermal Reservoir Engineering", Stanford U., Stanford, Ca. (January, 2005) 30.
19. Samaniego, V. F., Pulido, B. H., Rivera, R. J., Camacho, R., Perez, V. H. and and Martinez B.: "A Tracer Injection-Test Approach to Reservoir Characterization: Theory and Practice". International Petroleum Technology Conference, 21-23 November 2005, Doha, Qatar 11038-MS.
20. Abramowitz, M.: "*Handbook of Mathematical Functions with Graphs and Mathematical Tables*", U.S. Department of Commerce, National Bureau of Standards, Applied Mathematical Series 55, Washington D. C., 1964.
21. Bender, C. M. and Orszag, S. A.: Advanced Mathematical Methods for Scientists and Engineers, McGrawHill Book Company, USA, 1978, page 100.
22. Jogen K., Feder J., Boger F. and Jossang T., 1988: *Fractal structure of Hydrodinamic Dispersion in Porous Media*. Physical Review Letters, Volume 61, Number 26 (December).

APPENDIX A. CONDITIONS FOR AN INFINITE SYSTEM.

Initial condition: no exist tracer before injection.

$$C_f(r,0)=0 \tag{A-1}$$

Using the definition for dimensionless concentration for constant mass flux injection in the inner boundary:

$$C_{fD}\left(\frac{[r]}{r_w},\frac{\alpha_D\, a[0]}{r_w^{\,2}}\right)=\frac{D_r\, 2\pi\, hC_f(r,0)}{\dot{m}_w}$$

$$C_{fD}(r_D,0)=0 \tag{A-2}$$

Internal boundary condition: Constant mass flux production.

The mass flux is generated due to a gradient concentration caused by the flow toward a producing observation or measuring well, and it is proportional to the dispersion coefficient (Fick's law):

$$\dot{m}(r,t)=\frac{\partial G(r,t)}{\partial t}=-D_r A\frac{\partial C_f(r,t)}{\partial r} \tag{A-3}$$

The minus sign is due to the direction is the more to minus.

The mass flux per unit area (mass flux density) can be obtained from the previous Eq. A-3:

$$J_f(r,t)=\frac{-\dot{m}(r,t)}{A}=-D_r\frac{\partial C_f(r,t)}{\partial r} \tag{A-4}$$

Solving for the derivative of concentration:

$$\frac{\partial C_f(r,t)}{\partial r}=\frac{-\dot{m}(r,t)}{D_r A} \tag{A-5}$$

For the conditions at the injection well:

$$\frac{\partial C_f(r_w,t)}{\partial r}=\frac{-\dot{m}(r_w,t)}{D_r\, 2\pi r_w h} \tag{A-6}$$

Defining constant mass flux at the injection well:

$$\dot{m}(r_w,t)=\dot{m}_w \tag{A-7}$$

Substituting Eq. (A-7) in Eq. (A-6), the internal boundary condition for a continuous constant mass flux tracer injection is obtained:

$$\frac{\partial C_f(r_w,t)}{\partial r} = \frac{-\dot{m}_w}{D_r 2\pi r_w h} \quad \text{(A-8)}$$

Through the use of Eq. (27), this expression can be written in dimensionless form:

$$\frac{\dot{m}_w}{D_r 2\pi r_w h} \frac{\partial C_{fD}([r_w]/r_w,\ \alpha_D a[t]/r_w^2)}{\partial r_D} = \frac{-\dot{m}_w}{D_r 2\pi r_w h} \quad \text{(A-9)}$$

Simplifying is obtained the *Dimensionless internal boundary condition for constant mass flux*:

$$\frac{\partial C_{fD}(1,t_D)}{\partial r_D} = -1 \cdot \quad \text{(A-10)}$$

External boundary condition: infinite reservoir.

$$\lim_{r\to\infty} C_f(r,t) = 0 \quad \text{(A-11)}$$

$$\lim_{\substack{r\to\infty \\ r_m}} C_{fD}\left(\frac{[r]}{r_w}, \frac{\alpha_D a[t]}{r_w^2}\right) = \frac{D_r 2\pi h}{\dot{m}_w}\left[\lim_{r\to\infty} C_f(r,t)\right]$$

$$\lim_{r_D\to\infty} C_{fD}(r_D,t_D) = 0 \quad \text{(A-12)}$$

APPENDIX B. GENERAL SOLUTION IN LAPLACE SPACE FOR THE FLOW OF TRACERS IN NATURALLY FRACTURED RESERVOIRS

Applying the Laplace transform to equation (19), substituting the initial condition given by Eq. (20) and solving for the tracer concentration in the inaccessible matrix volume pore:

$$\overline{C}_{smD}(z_D,s) = \left[\frac{M_{mD}}{[1-f]s + M_{mD}}\right]\overline{C}_{mD}(z_D,s) \quad \text{(B-1)}$$

Applying the Laplace transform to the Eq. (15) and substituting the initial conditions (16) and (20):

$$D_{mD}\frac{d^2\overline{C}_{mD}(z_D,s)}{dz_D^2} - \lambda_D\overline{C}_{mD}(z_D,s) - [1-f]\,s\,\overline{C}_{smD}(z_D,s) = f\,s\,\overline{C}_{mD}(z_D,s) \quad \text{(B-2)}$$

Substituting Eq. (C-1) in Eq. (C-2):

$$\frac{d^2\overline{C}_{mD}(z_D,s)}{dz_D^2} - \frac{1}{D_{mD}}\left[\frac{\lambda_D}{s} + f + \frac{M_{mD}(1-f)}{[1-f]s + M_{mD}}\right]s\overline{C}_{mD}(z_D,s) = 0 \quad \text{(B-3)}$$

The general solution for flow in the matrix can be obtained solving Eq. (C-3):

$$\overline{C}_{mD}(z_D,s) = A\cosh\left(z_D\sqrt{sm(s)}\right) + B\sinh\left(z_D\sqrt{sm(s)}\right) \quad \text{(B-4)}$$

where:

$$m(s) = \frac{1}{D_{mD}}\left[\frac{[1-f]M_{mD}}{M_{mD} + s\,[1-f]} + f + \frac{\lambda_D}{s}\right] \quad \text{(B-5)}$$

Applying the Laplace transform to matrix boundary conditions Eqs. (17) and Eq. (18):

$$\overline{C}_{mD}(z_{Df},s) = \overline{C}_{fD}(r_D,s) \quad \text{(B-6)}$$

$$\frac{d\overline{C}_{mD}(z_{DH},s)}{dz_D} = 0 \quad \text{(B-7)}$$

Applying the boundary conditions is obtained to general equation for the matrix the equation that represents the tracer matrix concentration in function of the fracture concentration:

$$\overline{C}_{mD}(z_D,s) = \left[\frac{\cosh(z_0) - \tanh(z_H)\,\mathrm{senh}(z_0)}{\cosh(z_f) - \tanh(z_H)\,\mathrm{senh}(z_f)}\right]\overline{C}_{fD}(r_D,s) \quad \text{(B-8)}$$

where:

$$z_0 = z_D\sqrt{sm(s)} \quad \text{(B-9)}$$

$$z_f = z_{Df}\sqrt{sm(s)} \quad \text{(B-10)}$$

$$z_H = z_{DH}\sqrt{sm(s)} \quad \text{(B-11)}$$

The gradient concentration in the matrix block is obtained deriving Eq. (C-8), and the resulting expression at the fracture-matrix interface is:

$$\frac{d\overline{C}_{mD}(z_{Df},s)}{dz_D} = \sqrt{sm(s)}\left[\frac{\tanh(z_f) - \tanh(z_H)}{1 - \tanh(z_H)\tanh(z_f)}\right]\overline{C}_{fD}(r_D,s) \quad \text{(B-12)}$$

Applying the Laplace Transform to Eq. (11) and substituting the initial condition given by (12):

$$\frac{1}{r_D}\frac{d^2\overline{C}_{fD}(r_D,s)}{dr_D^2} - \frac{1}{\alpha_D r_D}\frac{d\overline{C}_{fD}(r_D,s)}{dr_D} - \lambda_D\overline{C}_{fD}(r_D,s) + \frac{1}{\sigma_D}\frac{d\overline{C}_{mD}(z_{fD},s)}{dz_D} = s\overline{C}_{fD}(r_D,s) \quad \text{(B-13)}$$

Substituting the Eq. (C-12) in Eq. (C-13):

$$\frac{1}{r_D}\frac{d^2C_{fD}(r_D,s)}{dr_D^2} - \frac{1}{\alpha_D r_D}\frac{dC_{fD}(r_D,s)}{dr_D} - [\lambda_D + s]C_{fD}(r_D,s) + \frac{\sqrt{sm(s)}}{\sigma_D}\left[\frac{\tanh(z_f) - \tanh(z_H)}{1 - \tanh(z_H)\tanh(z_f)}\right]\overline{C}_{fD}(r_D,s) = 0 \quad \text{(B-14)}$$

This may be written:

$$\frac{d^2\overline{C}_{fD}(r_D,s)}{dr_D^2} - \frac{1}{\alpha_D}\frac{d\overline{C}_{fD}(r_D,s)}{dr_D} - \beta(s)r_D\overline{C}_{fD}(r_D,s) = 0 \quad \text{(B-15)}$$

where:

$$\beta(s) = \frac{\sqrt{sm(s)}}{\sigma_D}\left[\frac{\tanh(z_H) - \tanh(z_f)}{1 - \tanh(z_H)\tanh(z_f)}\right] + \lambda_D + s \quad \text{(B-16)}$$

The general solution of the variables coefficients ordinary differential equation is given for Eq. (B-17):

$$\bar{C}_{fD}(r_D,\ s) = e^{\frac{r_D}{2\alpha_D}}\ \left[k_1\ A_i\ (Y_0) + k_2 Bi(Y_0)\right] \tag{B-17}$$

where:

$$Y_0 = \frac{r_D\beta(s)+1/4{\alpha_D}^2}{(\beta(s))^{2/3}} \quad . \tag{B-18}$$

APPENDIX C. INFINITE SOLUTION IN LAPLACE SPACE FOR THE FLOW OF TRACERS IN NATURALLY FRACTURED RESERVOIRS

Applying the Laplace transform to the boundary conditions given by Eq. (A-12) and (A-14):

$$\frac{d\ \bar{C}_{fD}(1,s)}{dr_D} = \frac{-1}{s} \tag{C-1}$$

$$\lim_{r_D\to\infty} \bar{C}_{fD}(r_D,s) = 0 \tag{C-2}$$

Applying the external boundary condition and considering that the Airy function Ai(x) for big arguments tend to zero, $k_2 = 0$ *in* Eq. (B-17).

Substituting the constant k_2 in Eq.(B-17):

$$\bar{C}_{fD}(r_D,s) = e^{\frac{r_D}{2\alpha_D}} k_1 Ai(Y_0) \tag{C-3}$$

where:

$$Y_0 = \frac{r_D\beta(s)+1/\left(4{\alpha_D}^2\right)}{\beta(s)^{2/3}} \tag{C-4}$$

Applying the internal boundary condition, k_1 can be expressed:

$$k_1 = \frac{-1}{s}\frac{e^{\frac{-1}{2\alpha_D}}}{\left[Ai(Y_1)/2\alpha_D + (\beta(s))^{1/3} Ai'(Y_1)\right]} \tag{C-5}$$

where:

$$Y_1 = \frac{\beta(s)+1/\left(4{\alpha_D}^2\right)}{\beta(s)^{2/3}} \tag{C-6}$$

Substituting this constant in the partial solution given by Eq. (C-3):

$$\bar{C}_{fD}(r_D,s) = \frac{e^{\frac{r_D-1}{2\alpha_D}}}{s}\left[\frac{-Ai(Y_0)}{Ai(Y_1)/2\alpha_D + (\beta(s))^{1/3} Ai'(Y_1)}\right] \tag{C-7}$$

where:

$$Y_0 = \frac{r_D\beta(s)+1/4{\alpha_D}^2}{\beta(s)^{2/3}} \tag{C-8}$$

$$Y_1 = \frac{\beta(s)+1/\left(4{\alpha_D}^2\right)}{\beta(s)^{2/3}} \tag{C-9}$$

The wellbore concentration:

$$\overline{C_{wD}}(s) = \bar{C}_{fD}(1,s) \tag{C-10}$$

The wellbore concentration:

$$\bar{C}_{wD}(s) = \frac{-1}{s\left[1/2\alpha_D + (\beta(s))^{1/3}\ Ai'(Y_1)/Ai(Y_1)\right]} \tag{C-11}$$

where:

$$Y_1 = \frac{\beta(s)+1/4{\alpha_D}^2}{\beta(s)^{2/3}} \tag{C-12}$$

$$\beta(s) = \frac{\sqrt{sm(s)}}{\sigma_D}\left[\frac{tanh(z_H)-tanh(z_f)}{1-tanh\ (z_H)\ tanh(z_f)}\right] + s + \lambda_D \tag{C-13}$$

$$m(s) = \frac{1}{D_{mD}}\left[\frac{[1-f]M_{mD}}{M_{mD}+s\,[1-f]} + f + \frac{\lambda_D}{s}\right] \tag{C-14}$$

Approximate Analytical solutions

For short times (large arguments $s \to \infty$):

When substituting practical values of Table 1 in the function m(s), Eq. C-14, presents an *almost* constant value (Fig. 4) and same case for several set of practical data:

$$m(s) \approx f / D_{mD} \approx {c_x}^2 \tag{C-15}$$

Then:

$$\sqrt{sm(s)} \approx c_x\sqrt{s} \tag{C-16}$$

The group that involve the slab geometry form of the matrix converge very fast to "one":

$$\frac{tanh\ (z_H) - tanh\ (z_f)}{1 - tanh\ (z_H)\ tanh\ (z_f)} \approx \frac{1 - z_f}{1 - [1]z_f} \approx 1 \tag{C-17}$$

Substituted C-16 and C-17 in $\beta(s)$, C-13:

$$\beta(s) \approx \frac{c_x}{\sigma_D}\sqrt{s}\,[1] + s + \lambda_D \tag{C-18}$$

Both the constant is very small, due to very high values of dimensionless sigma around the six order of constant and low values of dimensionless decay constant.

Then, when m(s) is substituted in $\beta(s)$, we obtain the behaviour for this function also shown in (Fig 4):

$$\beta(s) \approx s \tag{C-19}$$

That is the similar value for homogeneous case, is named "homogeneous in fractures":

For s tend to infinite, dominate the first term of "Y" function Eq. C-12:

$$Y_1 \approx (\beta(s))^{1/3} \quad \text{(C-20)}$$

Then substituting C-19 in C-20:

$$Y_1 \approx s^{1/3} \quad \text{(C-21)}$$

Using the ratio of the Airy function given by Eq. (C-22):

$$Ai'(Y_1)/Ai(Y_1) = -1.2e^{-Y_1^{\frac{1}{5}}} \quad \text{(C-22)}$$

Substituting (C-21) in C-22:

$$Ai'(s^{1/3})/Ai(s^{1/3}) = -1.2e^{-\left(s^{1/3}\right)^{\frac{1}{5}}} \quad \text{(C-23)}$$

Substituting Eq. C-21 and C-23 in Eq. (C-11):

$$\overline{C}_{wD}(s) = \frac{-1}{s\left[0.5/\alpha_D - 1.2s^{1/3}e^{-s^{1/15}}\right]} \quad \text{(C-24)}$$

For large s:

$$e^{-s^{1/15}} \approx 0.435s^{-1/9} \quad \text{(C-25)}$$

Substituting:

$$\overline{C}_{wD}(s) = \frac{-1}{s\left[0.5/\alpha_D - 0.522s^{1/3}s^{-1/9}\right]} \quad \text{(C-26)}$$

For large arguments ($s \to \infty$), this expression can be written as,

$$s\overline{C}_{wD}(s) = \frac{1}{0.522\left[s^{2/9} - 0.9/\alpha_D\right]} \quad \text{(C-27)}$$

The analytical inversion for **short times** of Eq. (C-11) is given by Eq. (C-28):

$$C_{wD}(t_D) = \frac{1}{0.522\Gamma(11/9)}\int_0^{t_D} {t_D}^{2/9} dt_D \quad \text{(C-28)}$$

$$C_{wD}(t_D) = \frac{9{t_D}^{11/9}}{11[0.522]0.677} = 0.432{t_D}^{11/9} \quad \text{(C-29)}$$

For large times (short arguments, $s \to 0$),
When substituting practical values of **Table 1** in the function m(s), Eq. C-14, presents an *almost* constant value and same case for several set of practical data:

$$m(s) \approx 1/D_{mD} \approx {c_x}^2 \quad \text{(C-30)}$$

Then:

$$\sqrt{sm(s)} \approx c_x\sqrt{s} \quad \text{(C-31)}$$

The group that involve the sphere geometry form of the matrix converge to:

$$\coth(z_f) - \frac{1}{z_f} \approx 20\sqrt{s} \quad \text{(C-32)}$$

Substituted C-31 and C-32 in $\beta(s)$:

$$\beta(s) \approx \frac{c_x}{\sigma_D}\sqrt{s}\left[20\sqrt{s}\right] + s + \lambda_D \quad \text{(C-33)}$$

Neglecting de dimensionless constant decay:

$$\beta(s) \approx \left[1 + \frac{20c_x}{\sigma_D}\right]s \approx s \quad \text{(C-34)}$$

That is the similar value for homogeneous case, is named "homogeneous in fractures":

For s tend to zero, dominate the second term of "Y" function Eq. C-12:

$$Y_1 \approx 0.25(\beta(s))^{-2/3}/{\alpha_D}^2 \quad \text{(C-35)}$$

Substituting Eqs. (C-34) in "Y" function

$$Y_1 \approx 0.25s^{-2/3}/{\alpha_D}^2 \quad \text{(C-36)}$$

Substituting C-36 in the relationship between Airy function and its derivative:

$$Ai'(Y_1)/Ai(Y_1) \approx -1.2e^{-Y_1^{1/5}} \quad \text{(C-37)}$$

$$= -1.2\left[\frac{0.25s^{-2/3}}{{\alpha_D}^2}\right]e^{-\left[\frac{0.25s^{-2/3}}{{\alpha_D}^2}\right]^{1/5}} \quad \text{(C-38)}$$

Substituting the relationship C-38 in C-11:

$$\overline{C}_{wD}(s) = \frac{-1}{s\left[0.5\alpha_D - 1.2\left[\frac{0.25s^{-2/3}}{{\alpha_D}^2}\right]e^{-\left[\frac{0.25s^{-2/3}}{{\alpha_D}^2}\right]^{1/5}}\right]} \quad \text{(C-39)}$$

For short s:

$$e^{-(0.25)^{1/5}s^{2/15}/{\alpha_D}^2} \approx 0.4685s^{-1/11{\alpha_D}^2} \quad \text{(C-40)}$$

Substituting Eq. (C-40) in Eq. (C-39):

$$\overline{C}_{wD}(s) = \frac{-{\alpha_D}^2}{s\left[0.5\alpha_D - 0.5622s^{-2/3}s^{-1/11{\alpha_D}^2}\right]} \quad \text{(C-41)}$$

For large times arguments ($s \to 0$),

$$\overline{C}_{wD}(s) = \frac{{\alpha_D}^2}{0.5622s\left[s^{-22/33} - 0.889\alpha_D\right]} \quad \text{(C-42)}$$

$$\overline{C}_{wD}(s) = \frac{{\alpha_D}^2}{0.5622\left[s^{1/3} - 0.889/\alpha_D s\right]} \quad \text{(C-43)}$$

In the denominator one term converge very fast to zero:

$$\overline{C}_{wD}(s) = \frac{{\alpha_D}^2}{0.5622\left[s^{1/3}\right]} \tag{C-44}$$

The analytical inversion for **large times** is expressed as follows:

$$C_{wD}(t_D) = \frac{{\alpha_D}^2 {t_D}^{1/3}}{0.5622\,\Gamma(1/3)} = 0.4{\alpha_D}^2 {t_D}^{1/3} \tag{C-45}$$

APPENDIX D. SOLUTIONS FOR CONSTANT MASS FLUX PULSE

A well is pulsed with cycles of injection followed by shut in. The concentration response to the cycles is then measured in an offset well.

The concepts involved are fairly straightforward. The bottom hole concentration in a shut in well will respond to injection cycles in an offset well. The magnitude and timing of the response depend on the mass flux, the dispersion that lie between the wells. Inhomogeneities, geometry and boundaries also affect the response, but these factors are not included in the scope of this paper.

For instance, if a well is injected for a time Δt, then shut in, by superposition in time, the concentration response in the shut in well is:

$$C_{wD}(t_D) = 0.4{\alpha_D}^2\left[{t_D}^{1/3} - (t_D - \Delta t_D)^{1/3}\right] \tag{D-1}$$

Going further, if there are a number of cycles of injection followed by shut-in, if each injection rate is equal, and if each cycle lasts for an eual period of time (Δt), Then by superposition in time the equation is:

$$C_{wD}(t_D) = 0.4{\alpha_D}^2\left[\sum_{n=0}^{N-1}(-1)^n (t_D - n\Delta t_D)^{1/3}\right] \tag{D-2}$$

Can be used the solution evaluated in $t_{pD} + \Delta t_D$ and resting the solution evaluated in Δt_D.

APPENDIX E. INTERNAL BOUNDARY CONDITIONS: PULSE MASS FLUX INJECTION.

The constant mass flux is changed by a pulse in A-10:

$$\dot{m}_w = M\delta(t_D) \tag{E-1}$$

Substituting Eq. E-1 in internal condition for constant mass flux:

$$\frac{\partial C_f(r_w, t)}{\partial r} = \frac{-M\delta(t)}{D_r\, 2\pi\, r_w h} \tag{E-2}$$

Substituting the derivate by a dimensionless derivate, using eq. 27:

$$\frac{\dot{m}_w}{D_r\, 2\pi\, r_w h}\frac{\partial C_{fD}(1, t_D)}{\partial r_D} = \frac{-M\delta(t_D)}{D_r\, 2\pi\, r_w h} \tag{E-3}$$

Simplifying is obtained the Dimensionless boundary condition for pulse mass flux

$$\frac{\partial C_{fD}(1,\ t_D)}{\partial r_D} = -T_0\delta(t_D) \tag{E-4}$$

where :

$$T_0 = \frac{M}{\dot{m}_p} = 1 \tag{E-5}$$

(Considering only one pulse)

Applying the Laplace transform to the inner boundary condition for a pulse mass flux given by Eq. (A-13):

$$\frac{d\,\overline{C}_{fD}(1, s)}{dr_D} = -1 \tag{E-6}$$

The solution for a constant mass flux pulse:

$$\overline{C}_{fD}(r_D, s)_{pulse} = e^{\frac{r_D - 1}{2}}\left[\frac{-Ai\ (Y_0)}{Ai\ (Y_1)/\,2\alpha_D + (\beta(s))^{1/3} Ai'\ (Y_1)}\right] \tag{E-7}$$

where:

$$Y_o = \frac{r_D\beta(s) + 1/\,4{\alpha_D}^2}{\beta(s)^{2/3}} \tag{E-8}$$

$$Y_1 = \frac{\beta(s) + 1/\,4{\alpha_D}^2}{\beta(s)^{2/3}} \tag{E-9}$$

The wellbore concentration for a constant mass flux pulse:

$$\overline{C}_{wD}(s)_{pulse} = \frac{-1}{1/\,2\alpha_D + (\beta(s))^{1/3} Ai'\ (Y_0)/\,Ai\ (Y_0)} \tag{E-10}$$

Comparing Eq. (E-10) with Eq. (C-11):

$$\overline{C}_{wD}(s)_{pulse} = s\overline{C}_{wD}(s) \tag{E-11}$$

The analytical inversion of Eq. (E-11):

$$C_{wD}(t_D)_{pulse} = \frac{dC_{wD}(t_D)}{dt_D} \tag{E-12}$$

From this expression we observe the known fact that the derivative of the continuous tracer injection solution yields the pulse injection solution (Chen, 1987).

Table 3. Practical values used in the evaluation of the *m(s)* function.

Q	h	a	α	M_m	D_m	λ	σ
m^3/D	m	M^2/H	m	1/s	m^2/s	1/s	Dim
2	200	0.04	0.5	0.500	$1.E^{-04}$	$1.E^{-06}$	0.032

ϕ_t	ϕ_{fb}	ϕ_{mb}	H	h_f	v_b	ϕ_{sm}	f=(ϕ_{mb} - ϕ_{sm})/ ϕ_{mb}
fraction	fraction	fraction	m	m	m^3	Dim	Dim
0.130	0.0169	0.1131	1.5	0.0085	3.43	0.01	0.89

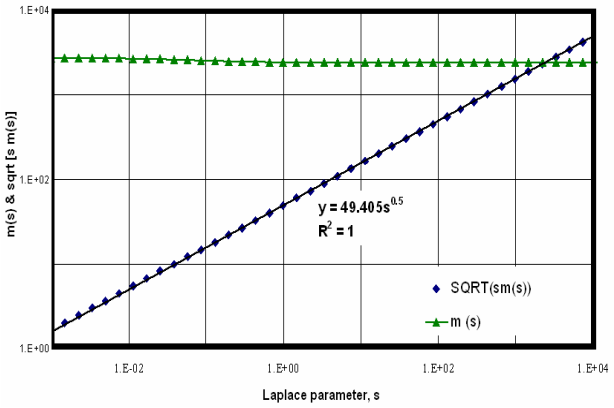

Fig. 3. The *m(s)* function is constant for several set of practical values; it only changes when the inaccessible pore volume is higher than 50%.

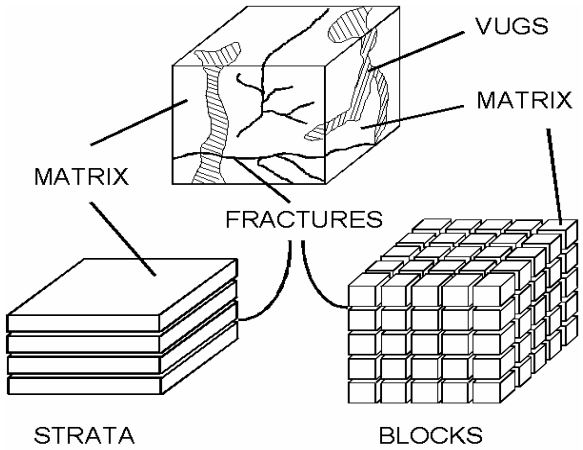

Fig. 1. Representation of a naturally fractured reservoir.

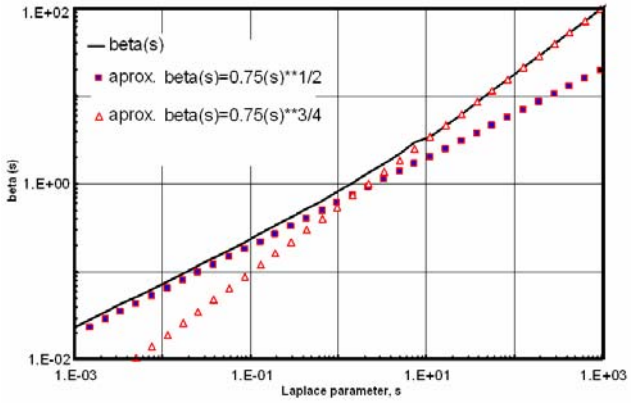

Fig. 4. Approximations for the Beta(s) function using the practical values of Table 1.

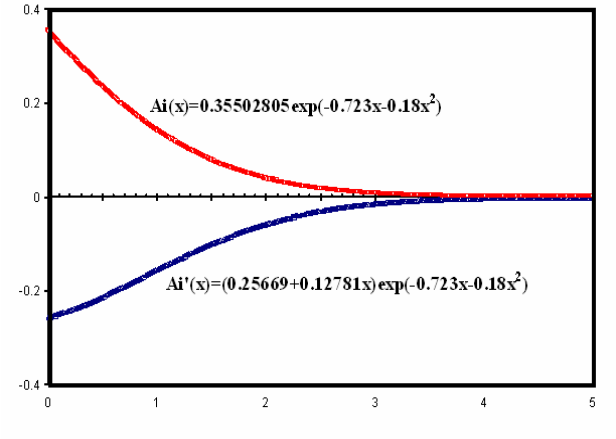

Fig. 2. A new approximation for Airy function and its derivative proposed compared with data of Abramowitz and Stegun.

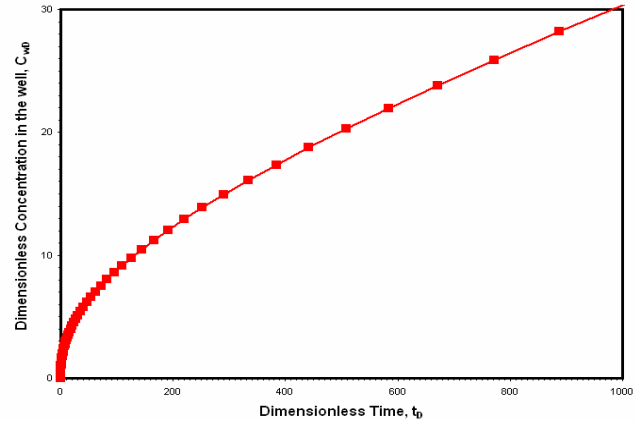

Fig. 5. Solutions for homogeneous continuous constant mass flux tracer injection, for radial flow in a cubic matrix naturally fractured reservoir with transient fracture-matrix transfer.

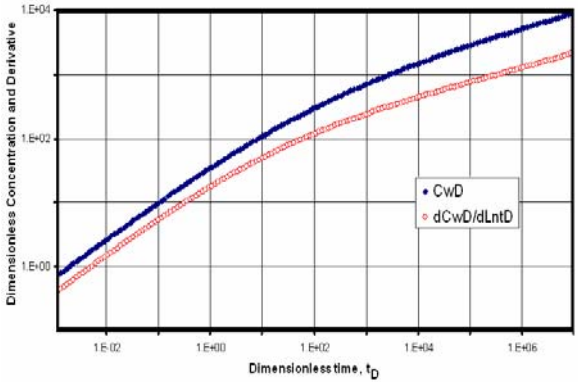

Fig. 6. Concentration and derivative tracer behaviors for homogeneous continuous constant mass flux tracer injection, for radial flow in a slabs naturally reservoir with transient fracture-matrix transfer.

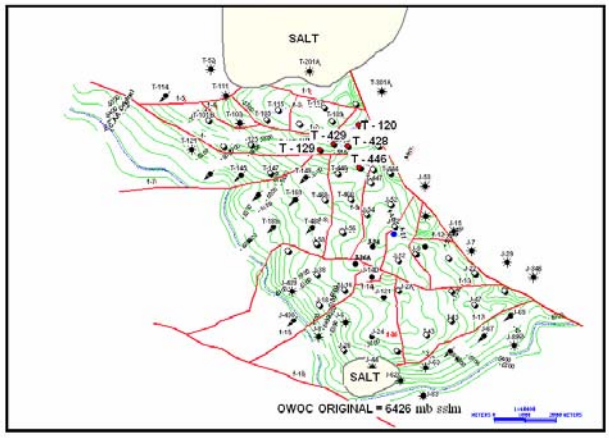

Fig. 7. Top of upper Jurassic kimmerigdian layer of the Jujo-Tecominoacán field, México.

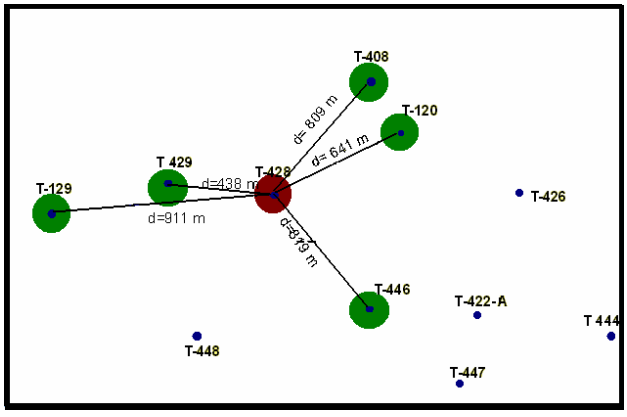

Fig. 8. Detailed areal view of the injection well T-428 and the tracer concentration measuring wells.

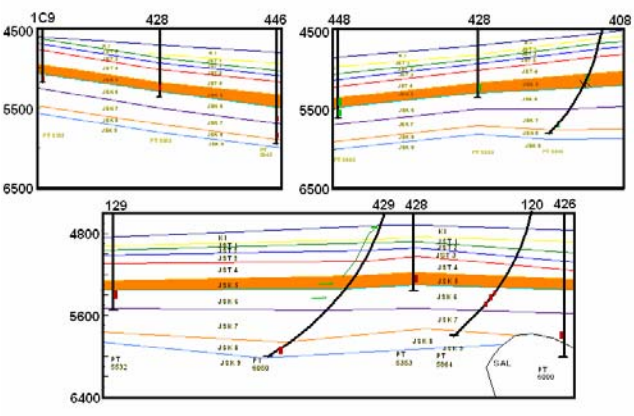

Fig. 9. Cross sections of the injection well T-428 and the tracer concentration measuring wells.

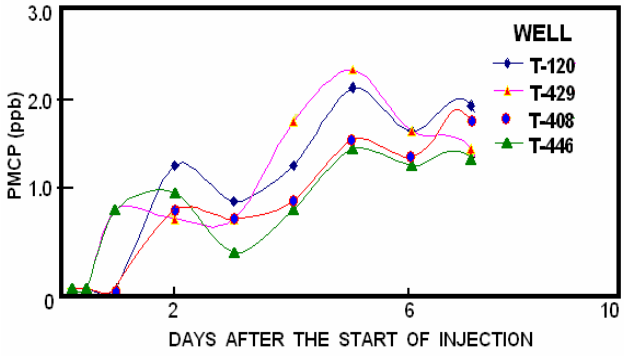

Fig. 10. Tracer concentrations vs. time for the injection test in well T-428, Jujo-Tecominoacán field, México.

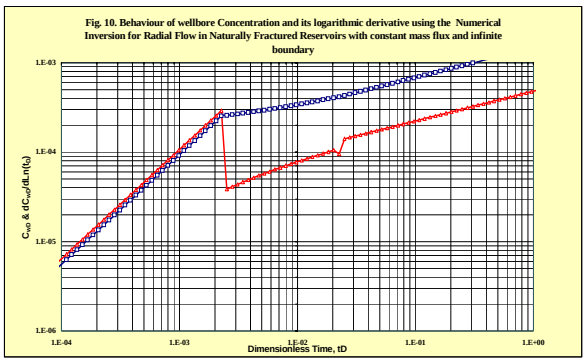

Fig. 11. Is observed a transition zone for interpretation and is obtained one value of *mixing coefficient* of 70 ft, several times that values defined in cores.